Macromolecules

pubs.acs.org/Macromolecules Article

Synthesis of Semiaromatic AA/BB-Type Polyamides via Chemoenzymatic Polycondensation

Yusuke Ueno, Kousuke Tsuchiya,* Hiroyasu Masunaga, and Keiji Numata*

Cite This: *Macromolecules* 2024, 57, 11658−11669 Read Online

ACCESS | Metrics & More | Article Recommendations | Supporting Information

ABSTRACT: Polypeptide-based AA/BB-type polyamides containing aromatic moieties in the main chains were synthesized via chemoenzymatic polycondensation of diamine and diester-type aromatic monomers through the use of papain in aqueous buffers. To mitigate the low substrate recognition of papain by aromatic units, aromatic diamines, such as 1,3-phenylenediamine (Pda), 2,4-diaminoanisole (Dan) and 2,4-diaminophenol (Dap), and aromatic diacids, such as 5-aminoisophthalic acid (Aip), were modified with glycine. The diamine monomers GlyPdaGly, GlyDanGly and GlyDapGly and diester monomer GlyAipGly were used for polycondensation in the presence of papain, resulting in the formation of the AA/BB-type polyamides poly(GlyPdaGly-*alt*-GlyAipGly) (AP(GG)), poly(GlyDanGly-*alt*-GlyAipGly) (AP(GG)^{OMe}) and poly(GlyDapGly-*alt*-GlyAipGly) (AP(GG)^{OH}). Structural analysis of the polyamides via Fourier transform infrared (FT-IR) spectroscopy and wide-angle X-ray diffraction (WAXD) revealed that the AP(GG) series was largely amorphous, resulting from a reduction in the hydrogen bonding of PolyGly due to the inclusion of aromatic moieties in the main chain. Thermal analysis of the AP(GG) series revealed high thermal stability and thermoplasticity, which are caused by the rigid structure of the benzene ring and the amorphous structure of the polyamides. The postpolycondensation products of AP(GG), AP(GG)^{OMe} and AP(GG)^{OH} formed hyperbranched/networked structures via amidation of Aip amines. Notably, chemoenzymatic polymerization followed by postpolycondensation provided peptide-based semiaromatic polyamides with high thermal stability.

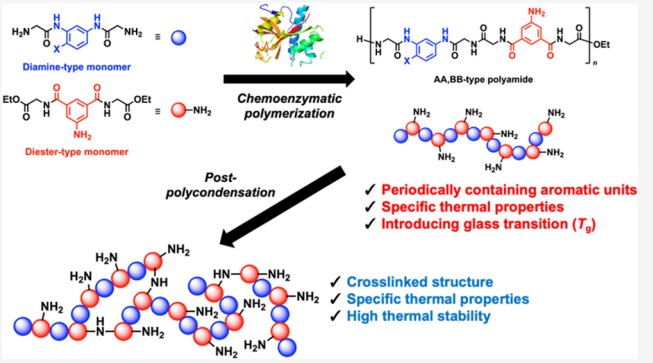

INTRODUCTION

Biopolymers originating from natural living organisms are environmentally friendly materials with negligible effects on carbon dioxide emissions and are promising as sustainable alternatives to petroleum-based materials. Proteins and polypeptides are biodegradable biopolymers that exhibit various properties depending on their amino acid sequences. Designing appropriate amino acid sequences provides diverse functionalities of artificial polypeptide materials. Structural proteins such as silk fibroin, elastin, and resilin exhibit a wide range of mechanical properties achieved by self-assembly of specific peptide motifs. For example, the extraordinary strength and toughness of spider silks rely on a crystalline region formed by polyalanine motifs and an amorphous region formed by glycine-rich motifs in spider silk proteins.[1,2] Artificial polypeptide materials have been developed to imitate the material properties of structural proteins by assembling specific peptide motifs extracted from protein sequences.[3,4]

Polypeptides undergo self-assembly via noncovalent interactions such as hydrogen bonding. Therefore, polypeptide materials generally exhibit poor solubility and the absence of a melting point below their thermal decomposition temperature due to multiple hydrogen bonds, which restricts their practical application to bulk materials. Very few studies have been reported for thermally processable artificial proteins/polypeptides to date.[5,6] To endow artificial polypeptide materials with unique functions, the introduction of unnatural structures into polypeptide backbones has been demonstrated. Previous studies indicated that the introduction of synthetic polyamide units, such as nylon and aramid, yielded unprecedented properties derived from artificial primary and secondary structures.[7−11] In particular, the introduction of aromatic units into the polypeptide backbone resulted in specific artificial helical or sheet structures distinct from conventional α-helix and β-sheet structures.[7,9,10]

Chemoenzymatic polymerization is a green synthesis method for polypeptides that entails the utilization of proteases to catalyze peptide bond formation from amino acid ester monomers.[12] This method provides several advantages over conventional polypeptide synthesis methods, including solid-

Received: September 5, 2024
Revised: November 13, 2024
Accepted: November 15, 2024
Published: November 22, 2024

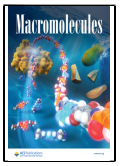

phase peptide synthesis, such as green conditions using aqueous media, atom economy, facile scalability, and regio- and stereoselective synthesis. Chemoenzymatic polymerization can also generate periodic polypeptides by using oligopeptide esters as monomers, even with the introduction of an artificial amino acid into the monomer sequence. Artificial amino acid esters, such as ω-aminoalkanoic acid and aminobenzoic acid derivatives, cannot be polymerized by protease-catalyzed polymerization, while the chemoenzymatic polymerization of tripeptides comprising both natural and artificial amino acids can provide corresponding polypeptides with the periodic insertion of artificial amino acid residues.[7,13]

Numerous aromatic polyamides have been synthesized via polycondensation of aromatic diamine and diester monomers, which provide AA/BB-type polyamides for various applications.[14] The combination of aromatic diamine and diester monomers results in a wide structural variety depending on the monomer structure. Previously, we synthesized amino acid–based diester derivatives from succinic acid and applied them in chemoenzymatic polymerization to propagate polypeptide chains from the two ester moieties, yielding telechelic-type polypeptides. Amino acid–based diester derivatives have been recognized by proteases in chemoenzymatic polymerization but have never been applied in AA/BB-type polycondensation catalyzed by proteases. In the case of polyester synthesis, there are several reports on lipase-catalyzed AA/BB-type polymerization of diester and diol monomers to yield semiaromatic polyesters.[15,16] However, these chemoenzymatic syntheses of polyesters entail the adoption of organic solvents and high temperatures.

In this study, we designed diamine and diester monomers containing both aromatic units and amino acid units for chemoenzymatic polymerization. The amine or carboxylic acid groups of aromatic units were modified with glycine derivatives to produce glycine-terminated diamine and diester monomers. Papain-catalyzed polymerization of glycine-terminated aromatic monomers successfully yielded the corresponding semiaromatic polyamides. The resulting semiaromatic polyamides exhibited glass transition temperatures, indicating that they are promising polypeptide-based materials with thermal processability.

EXPERIMENTAL SECTION

Materials. Papain was purchased from Merck Millipore (Burlington, Massachusetts) and used as received (EC number: 3.4.22.2). The activity was approximately 30,000 USP units mg^{-1}, where one unit was defined and adopted by the United States Pharmacopeia. Moreover, 1-(3-(dimethylamino)propyl)-3-ethylcarbodiimide hydrochloride (EDC·HCl) and ethyl cyano-(hydroxyimino)acetate (OxymaPure) were purchased from Watanabe Chemical Industries, Ltd. (Hiroshima, Japan), and used as received. The other chemicals were purchased from FUJIFILM Wako Pure Chemical Corporation (Tokyo, Japan) or Tokyo Chemical Industry Co., Ltd. (Tokyo, Japan), and they were used as received without purification unless otherwise noted.

Synthesis of GlyPdaGly·2HCl. *N-tert*-Butyloxycarbonyl (Boc)-glycine (40 mmol, 7.00 g), OxymaPure (40 mmol, 5.68 g), 1,3-phenylenediamine (Pda, 20 mmol, 2.16 g) and triethylamine (TEA, 35 mL) in dichloromethane (DCM, 40 mL) were added to a flask equipped with an addition funnel and a stir bar at −10 °C under nitrogen protection. A solution of EDC·HCl (40 mmol, 7.67 g) in DCM (40 mL) was added dropwise over 30 min, and the resulting mixture was stirred at −10 °C for 30 min and then at 25 °C for 24 h. The mixture was subsequently washed with 4% $KHSO_4$ aq (3 × 100 mL), sat. $NaHCO_3$ aq (3 × 100 mL) and saltwater in sequence. The organic layer was dried with Na_2SO_4 and concentrated via a rotary evaporator. The product was dried in vacuo to yield Boc-GlyPdaGly-Boc as a pale-brown solid. The obtained Boc-GlyPdaGly-Boc was then subjected to deprotection of the Boc groups. The crude product was then dissolved in DCM (40 mL), and trifluoroacetic acid (TFA, 40 mL) was added to the solution. The mixture was stirred at 25 °C for 2 h. After the solvent was removed under reduced pressure, the crude product was dissolved in a dioxane/HCl solution (4.0 M, 5 mL). The solution was subsequently poured into diisopropyl ether. The precipitate was filtered, washed with diisopropyl ether, and dried under vacuum to obtain GlyPdaGly·2HCl as a pale yellow solid. The yield was 4.58 g (77.7%). All other diamine-type tripeptide monomers were prepared via the same experimental procedure.

Synthesis of GlyAipGly·HCl. A solution of di-*tert*-butyl dicarbonate (55 mmol, 12.0 g) in methanol (40 mL) and TEA (20 mL) was added to a solution of 5-aminoisophthalic acid (Aip, 50 mmol, 9.06 g) in methanol (40 mL) at 25 °C. The mixture was stirred at 25 °C for 24 h. The solvent was removed under reduced pressure to yield Boc-Aip as a white solid. Then, Boc-Aip (20 mmol, 5.63 g), OxymaPure (40 mmol, 5.68 g), Gly-OEt·HCl (40 mmol, 5.58 g) and TEA (35 mL) in DCM (40 mL) were added to a flask equipped with an addition funnel and stir bar at −10 °C under nitrogen protection. A solution of EDC·HCl (40 mmol, 7.67 g) in DCM (40 mL) was added dropwise over 30 min, and the resulting mixture was stirred at −10 °C for 30 min and then at 25 °C for 24 h. The mixture was subsequently washed with 4% $KHSO_4$ aq (3 × 100 mL), sat. $NaHCO_3$ aq (3 × 100 mL) and saltwater in sequence. The organic layer was dried with Na_2SO_4 and concentrated via a rotary evaporator. The product was dried in vacuo to yield Gly(Boc-Aip)Gly as a pale-brown solid. The obtained Gly(Boc-Aip)Gly was then subjected to deprotection of the Boc group. The crude product was then dissolved in DCM (40 mL), and TFA (40 mL) was added to the solution. The mixture was stirred at 25 °C for 2 h. After the solvent was removed under reduced pressure, the crude product was dissolved in a dioxane/HCl solution (4.0 M, 5 mL). The solution was subsequently poured into diisopropyl ether. The precipitate was filtered, washed with diisopropyl ether, and dried under vacuum to obtain GlyAipGly·HCl as a pale yellow solid. The yield was 1.70 g (21.9%).

General Procedure of Chemoenzymatic Polymerization. GlyPdaGly·2HCl (0.30 mmol, 88.6 mg), GlyAipGly·HCl (0.30 mmol, 116.2 mg) and 1 M tris(hydroxymethyl)aminomethane (Tris) buffer (2 mL, pH 9.0) were added to a 10 mL glass tube equipped with a stir bar, and the mixture was stirred at 40 °C until all the substrates were completely dissolved. The pH of the monomer mixture reached 8.0. The monomer mixture was poured into a glass tube containing a magnetic stir bar, placed in a reaction device (ChemiStation, AYELA, Tokyo, Japan) at 40 °C and stirred at 800 rpm. Papain powder (100 mg, 50 mg mL^{-1}) was then added to the monomer solution to start the polymerization reaction. The mixture was stirred at 40 °C and 800 rpm for 6 h. After cooling to room temperature, the precipitate was collected via centrifugation at 9000 rpm and 4 °C for 15 min. The crude product was washed 3 times with deionized water and dried under vacuum to obtain the corresponding polypeptide AP(GG) as a brown powder. The yield was 71.8 mg (49.8%). The chemical structure of the product was characterized via proton nuclear magnetic resonance (^{1}H NMR) spectroscopy and matrix-assisted laser desorption/ionization time-of-flight mass spectrometry (MALDI-TOF MS). All other diamine-type monomers were also synthesized via the same experimental procedure.

Synthesis of PolyGly. Gly-OEt·HCl (3.0 mmol, 418.7 mg) and 1 M Tris buffer (3 mL, pH 9.0) were added to a 10 mL glass tube equipped with a stir bar, and the mixture was stirred at 40 °C until all the substrates were completely dissolved. The pH of the monomer mixture reached 8.0. The monomer mixture was poured into a glass tube containing a magnetic stir bar, placed in a reaction device (ChemiStation, AYELA, Tokyo, Japan) at 40 °C and stirred at 800 rpm. Papain powder (150 mg, 50 mg mL^{-1}) was then added to the monomer solution to start the polymerization reaction. The mixture was stirred at 40 °C and 800 rpm for 6 h. After cooling to room temperature, the precipitate was collected via centrifugation at 9000

https://doi.org/10.1021/acs.macromol.4c02125
Macromolecules 2024, 57, 11658−11669

Scheme 1. Papain-Catalyzed Polymerization of Aromatic-Containing Diamine and Diester Monomers

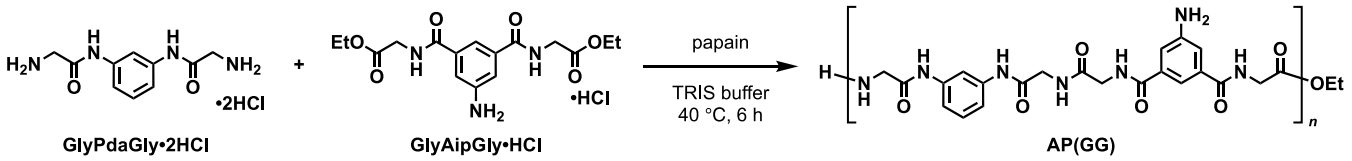

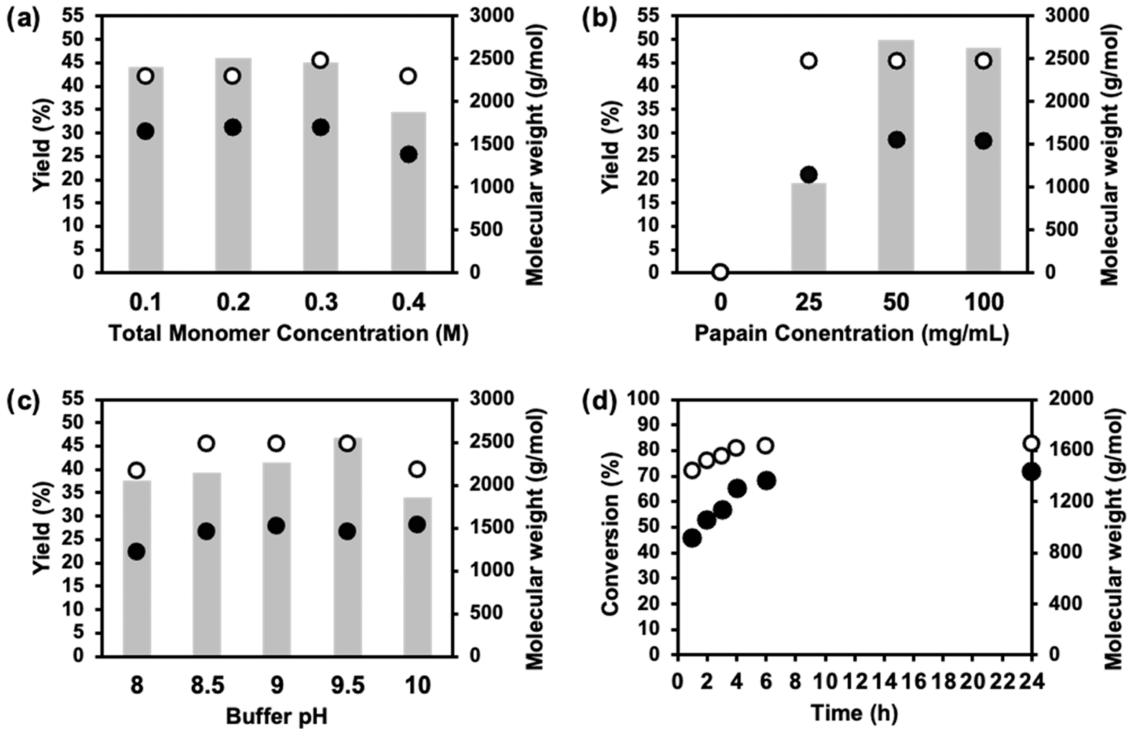

Figure 1. Optimization analysis of the synthesis of AP(GG) via papain-catalyzed polymerization. Effects of (a) the total monomer concentration, (b) papain concentration, and (c) buffer pH on the yield and molecular weight of the obtained polyamide. The bars denote the yields, and M_{max} and M_n are plotted as open and close circles, respectively. Conditions: (a) Papain concentration: 50 mg mL^{-1}, pH 9.0; (b) monomer concentration: 0.3 M, pH 9.0; (c) monomer concentration: 0.3 M, papain concentration: 50 mg mL^{-1}. (d) Time course of the conversion of GlyAipGly (open circles) and M_n (closed circles) under optimized conditions (monomer concentration: 0.3 M; papain concentration: 50 mg mL^{-1}; pH: 9.0).

rpm and 4 °C for 15 min. The crude product was washed 3 times with deionized water and dried under vacuum to obtain the corresponding PolyGly as a white powder. The yield was 75.6 mg (44.2%). The chemical structure of the product was characterized via MALDI-TOF MS (Figure S5).

Postpolycondensation of AP(GG). A solution of AP(GG) (50 mg) in *N*,*N*-dimethylacetamide (DMAc, 1 mL) was added to polyphosphoric acid (PPA, M_n = 14,100, 70 mg) in a 10 mL glass tube equipped with a stir bar and a stopcock under nitrogen protection. The solution was stirred at 120 °C for 24 h under nitrogen. After cooling to room temperature, the mixture was poured into water and stirred for 1 h. The precipitate was collected via centrifugation at 9,000 rpm and 4 °C for 15 min. The crude product was washed with deionized water, centrifuged 3 times, and lyophilized to produce a brown powder.

^{1}H NMR Spectroscopy. ^{1}H NMR spectra were recorded with a Bruker DPX400 spectrometer (Bruker, Bremen, Germany) at 400 MHz. Deuterated dimethyl sulfoxide (DMSO-d_6) was used as the solvent, and tetramethylsilane (TMS) served as an internal standard for the polypeptides.

Matrix-Assisted Laser Desorption/Ionization Time-of-Flight Mass Spectrometry (MALDI-TOF MS). MALDI-TOF MS spectra were recorded with an AutoFlex III Plus (Bruker) spectrometer using α-cyano-4-hydroxycinnamic acid (α-CHCA) as the matrix dissolved in acetonitrile.

Fourier Transform Infrared (FT-IR) Spectroscopy. The FT-IR spectra of the collected precipitate samples were recorded via an IR Prestige-21 Fourier transform infrared spectrophotometer (Shimadzu Corporation, Kyoto, Japan) with a MIRacle A single-reflection attenuated total reflection unit using a Ge prism.

Thermal Analyses. Thermogravimetric analysis (TGA) of the polymer samples was performed via a TGA/DSC2 instrument (Mettler Toledo, Columbus, OH). The polymer sample (~5 mg) was weighed in an aluminum pan and heated with an empty reference cell at a heating rate of 20 °C min^{-1} from 30 to 500 °C under nitrogen protection. Differential scanning calorimetry (DSC) measurements of the polypeptide samples were performed via a DSC 8500 instrument (PerkinElmer, Waltham, MA). The polypeptide sample (~5 mg) was weighed in an aluminum pan and subjected to heating/cooling cycles at a heating rate of 20 °C min^{-1} and a cooling rate of 100 °C min^{-1} over the range from −50 to 250 °C under nitrogen protection.

Gel Permeation Chromatography (GPC). GPC was performed via a JASCO HPLC system (PU-2086, DG2080−54, AS-2057, CO-2065; JASCO, Tokyo, Japan) with a Shodex KD-804 column (Showa Denko K. K., Tokyo, Japan) and a UV detector (UV-2075, JASCO). The polymer samples (2 mg mL^{-1}) eluted with 1-methyl-2-pyrrolidone (NMP) containing 10 mM lithium bromide were measured at a flow rate of 1.0 mL min^{-1}. The number (M_n) and weight-average molecular weights (M_w) and the molecular weight

https://doi.org/10.1021/acs.macromol.4c02125
Macromolecules 2024, 57, 11658−11669

Scheme 2. Synthesis of AP(GG)^{OMe} and AP(GG)^{OH} via Papain-Catalyzed Polymerization

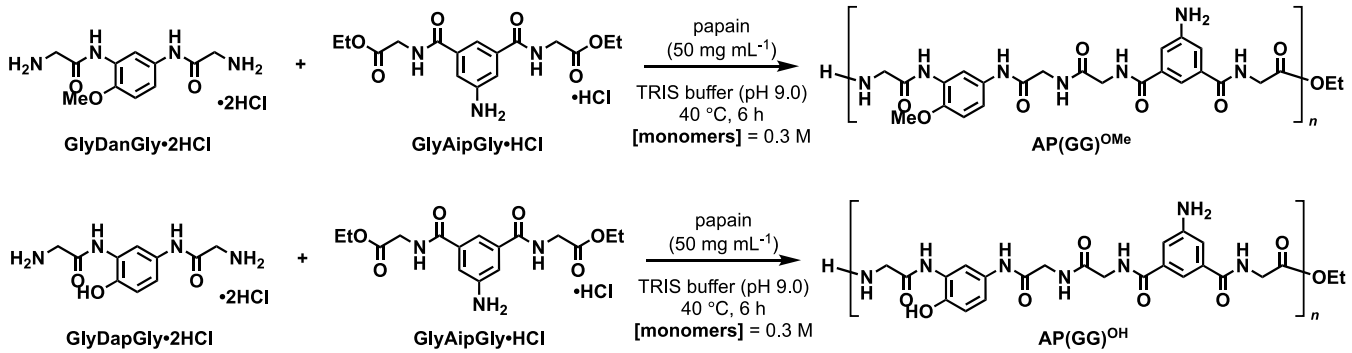

distribution (M_w/M_n) were estimated via polystyrene standards of the following molecular weights: 1.22×10^3, 2.98×10^3, 6.94×10^3, 1.83×10^4, 4.72×10^4 and 1.24×10^5.

Wide-Angle X-ray Diffraction (WAXD) Measurements. The synchrotron WAXD measurements of the polypeptide powdery samples were performed at the BL05XU beamline (SPring-8, Harima, Japan) using an X-ray energy of 12.4 keV (wavelength: 0.1 nm) with an automated sample changer. A beam with a diameter of 45 μm was employed. The obtained two-dimensional (2D) diffraction patterns were converted into one-dimensional (1D) profiles via azimuthal integration in Fit2D.

Heat Pressing. Heat pressing was performed via a Mini Test Press-SNH (Toyo Seiki, Tokyo, Japan). A 100 mg sample of the powdered material was placed in a mold (10 mm square) made from a 1 mm thick Teflon sheet, with Teflon sheets covering the top and bottom surfaces. The sample was then compressed at 210 °C and 10 MPa for 30 min, forming a 1 mm thick film.

RESULTS AND DISCUSSION

Previously, chemoenzymatic polymerization of aromatic unit-containing oligopeptide esters was successfully conducted in the presence of papain to obtain polyamides periodically containing 4-aminobenzoic acid units.[7] The modification of natural amino acids such as glycine and alanine mitigated the mismatch in the affinity of the aromatic units to the substrate pocket of papain, allowing the polymerization of artificial aromatic monomers. As shown in Scheme 1, we designed novel amino acid-modified monomers containing an aromatic diamine and aromatic diester for enzyme-mediated AA/BB-type polycondensation. As an amino acid moiety, we connected glycine residues to the termini of both Pda and Aip to synthesize diamine and diester monomers, namely, GlyPdaGly and GlyAipGly, respectively. Papain was selected as the polymerization catalyst because the glycine moiety is a suitable substrate for papain-mediated chemoenzymatic polymerization. Papain-catalyzed polymerization of GlyPdaGly and GlyAipGly was performed in Tris buffer at 40 °C (Scheme 1). As the polymerization proceeded, the corresponding polyamide AP(GG) gradually formed a precipitate. The precipitated product was insoluble in water, methanol and chloroform, whereas it was soluble in highly polar solvents such as DMSO and NMP, and fluorinated solvents such as hexafluoroisopropanol (HFIP) (Table S1).

Table 1. Papain-Catalyzed Polymerization of GlyAipGly with Various Diamine Monomers

diamine	polymer	yield[a] (%)	DP_{max}[b]	M_n[c]
GlyPdaGly	AP(GG)	49.8	5	1560
GlyDanGly	AP(GG)^{OMe}	26.7	4	1520
GlyDapGly	AP(GG)^{OH}	44.1	3	1130

[a]Precipitate was collected via centrifugation, washed with water, and lyophilized. [b]Determined via MALDI-TOF MS. DP: Degree of polymerization. [c]Determined from the ^{1}H NMR spectra.

The effects of the monomer and enzyme concentrations, buffer pH, and reaction time on the yield and molecular weight were investigated to optimize papain-catalyzed AA/BB-type polymerization. A summary of the results is shown in Figure 1. Because the monomer was saturated at a total monomer concentration over 0.4 M, we conducted the polymerization at concentrations ranging from 0.1 to 0.4 M. When the monomer concentration was varied, the yield and the maximum molecular weight (M_{max}) detected via MALDI-TOF MS were maximized at 0.2 M (46%) and 0.3 M (2,480 g mol^{-1}), respectively (Figures 1a and S1). M_n determined from the ^{1}H NMR spectra exhibited a similar tendency to that of M_{max}. Increasing the monomer concentration to 0.4 M slightly decreased the yield and molecular weight. This reduced polymerization efficiency at 0.4 M can be attributed to a relative shortage of papain available for binding monomer. As a result, unreacted monomers remained, or oligomers with very low molecular weight are formed.[17] The effect of the papain concentration was also examined, as shown in Figures 1b and S2. The polyamide AP(GG) was not obtained in the absence of papain, indicating that thermal polymerization did not occur under these mild conditions. The yield of the precipitate increased with increasing papain concentration and stabilized above 100 mg mL^{-1} papain.

The yield and molecular weight at different buffer pH values ranging from 8.0 to 10.0 were investigated for polymerization at the optimized monomer and papain concentrations (Figure 1c). The yield increased to 45% at pH 9.5, whereas the molecular weight was maximized at pH 9.0. The increase in pH yielded the optimum papain pH for proteolysis (6.0−7.0)[17,18] and facilitated competing hydrolysis of the obtained polyamide, resulting in a decrease in the molecular weight (Figure S3).

A time course experiment was conducted under the optimized conditions (monomer concentration: 0.3 M; papain concentration: 50 mg mL^{-1}; pH: 9.0). The conversion of GlyAipGly was monitored by ^{1}H NMR spectroscopy during polymerization (Figure 1d). The molecular weight reached 910 g mol^{-1} within 1 h and gradually increased with increasing polymerization time. After 6 h of reaction, the molecular weight was 1,370 g mol^{-1}, and no difference was observed up to a reaction time of 24 h. As shown in the MALDI-TOF MS spectra of AP(GG) after 24 h of polymerization (Figure S4),

https://doi.org/10.1021/acs.macromol.4c02125
Macromolecules 2024, 57, 11658−11669

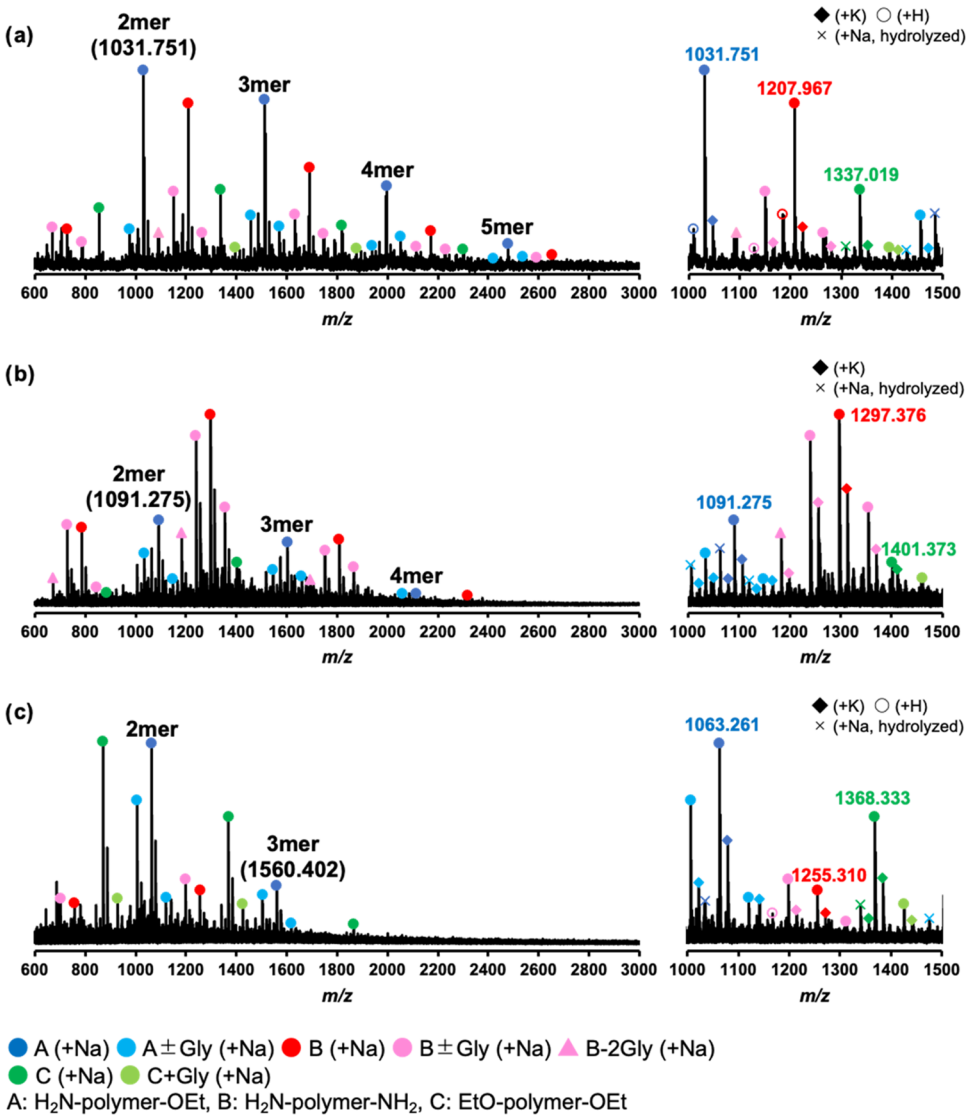

Figure 2. MALDI-TOF MS spectra of (a) AP(GG), (b) AP(GG)^{OMe}, and (c) AP(GG)^{OH} obtained via papain-catalyzed polymerization.

longer polymerization times facilitated hydrolysis and transamidation as side reactions. Therefore, 6 h of reaction was defined as the optimum time because the molecular weight was maximized, and side reactions were less likely to occur after 6 h.

Polymerization was attempted using other monomers to extend the structural variety of the polyamide. Two different types of aromatic diamine units, namely, 2,4-diaminoanisole (Dan) and 2,4-diaminophenol (Dap), were selected and converted into glycine-modified monomers GlyDanGly and GlyDapGly, respectively. Papain-catalyzed polymerization of GlyAipGly with GlyDanGly or GlyDapGly was performed under the optimized conditions (Scheme 2). The results are summarized in Table 1. Both GlyDanGly and GlyDapGly can polymerize with GlyAibGly in the presence of papain to yield the corresponding polyamides, namely, AP(GG)^{OMe} and AP(GG)^{OH}, respectively. The molecular weights of AP(GG)^{OMe} and AP(GG)^{OH} were estimated via ^{1}H NMR as 1,520 and 1130 g mol^{-1}, respectively. Owing to the relatively poor solubility of GlyDapGly units, AP(GG)^{OH} generally precipitated at an earlier polymerization stage, resulting in a lower molecular weight than those of AP(GG) and AP(GG)^{OMe}.

Papain-catalyzed AA/BB-type polycondensation was confirmed via MALDI-TOF MS. In the MALDI-TOF MS spectra of the polyamides, a series of peaks with m/z intervals of 481, 511, and 497 were detected for AP(GG), AP(GG)^{OMe}, and AP(GG)^{OH}, respectively (Figure 2). These values were identical to the molecular mass of one repeating unit (diamine + diester) for each polyamide, indicating that the aromatic units were periodically introduced into these polyamides. Three types of terminal combinations (type A: amine−ester; type B: amine−amine; and type C: ester−ester) were detected in terms of structural variety. The amine−ester terminal combination was mainly formed for AP(GG), whereas the amine−amine terminal combination dominated for AP(GG)^{OMe}. Amine−ester and ester−ester terminal combinations were mostly found for AP(GG)^{OH}. The solubility of the diamine monomers may be a contributing factor: GlyDapGly is less soluble than the other two diamine monomers, resulting in a relatively low concentration in solution, while GlyDanGly is more soluble, leading to a comparatively higher concentration. Furthermore, the additional insertion/deletion of glycine

https://doi.org/10.1021/acs.macromol.4c02125
Macromolecules 2024, 57, 11658−11669

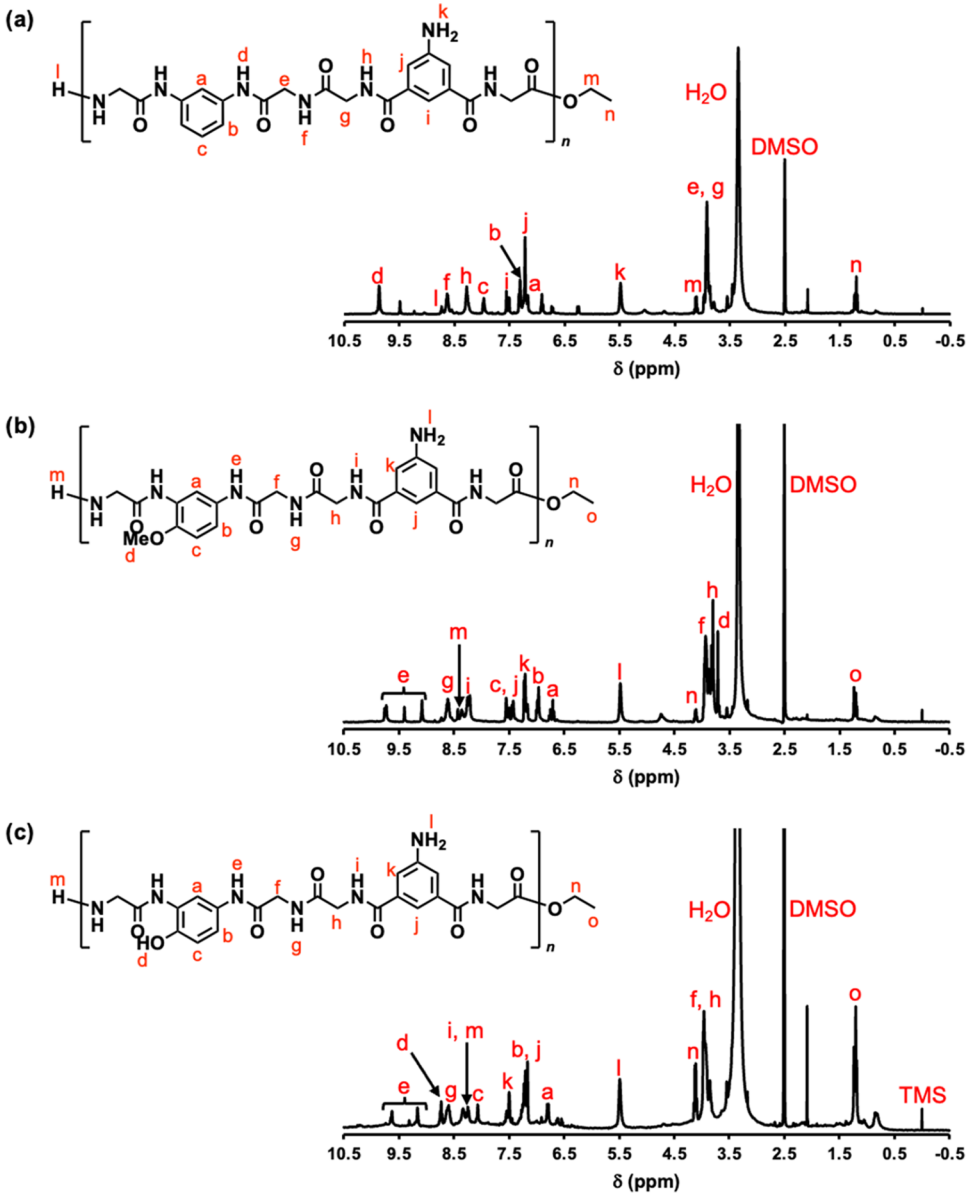

Figure 3. ^{1}H NMR spectra of (a) AP(GG), (b) AP(GG)^{OMe}, and (c) AP(GG)^{OH} in DMSO-d_6.

unit(s) was confirmed in all the polyamides as a minor series of peaks. The glycine unit migrated via putative transamidation (17−25%, calculated from ^{1}H NMR spectra) during polymerization, as described in previous studies.[19,20] AP(GG) exhibited the highest molecular mass, and the degree of polymerization (DP) reached as high as 5.

This polymerization method produced only low molecular weights and DP, resulting in the formation of oligomers rather than the high molecular weight polymers typically required for structural and bulk material applications. This is likely due to the inhibition of polymerization caused by the precipitation of the polymer from the aqueous solvent, as well as the inactivation of the C-terminal ester group by competing hydrolysis during the polymerization.

The chemical structures of the polyamides were characterized via the ^{1}H NMR and FT-IR spectroscopy techniques. In the ^{1}H NMR spectra, all the polymers showed signals assignable to aromatic protons from the Pda (Dan, Dap) and Aip moieties within the 6.5−7.5 ppm range (Figure 3). All the signals were assigned to the corresponding polyamides, confirming the periodic introduction of aromatic units into the polyamide backbones. The aromatic amine of the Aip moiety was assigned to the signal at 5.5 ppm for all the polyamides. This result indicates that enzyme-catalyzed condensation proceeded selectively between the amine and ester groups of the glycine residues and that the aromatic amine group of the Aip moiety remained intact during polymerization.

The FT-IR spectra of the polyamides are shown in Figure 4. Compared with the FT-IR spectra of polyglycine (PolyGly), a new peak assignable to the C═C stretching vibration mode emerged at 1600 cm^{-1} in the FT-IR spectra of the polyamides containing aromatic units compared with those of PolyGly, indicating that the aromatic units were incorporated into the polyamide backbones. The amide I peak at 1646 cm^{-1} corresponds to the stretching vibration mode of the carbonyl groups of the polyamides containing aromatic units. The amide I band reflects the effect of hydrogen bonding in the secondary

https://doi.org/10.1021/acs.macromol.4c02125
Macromolecules 2024, 57, 11658−11669

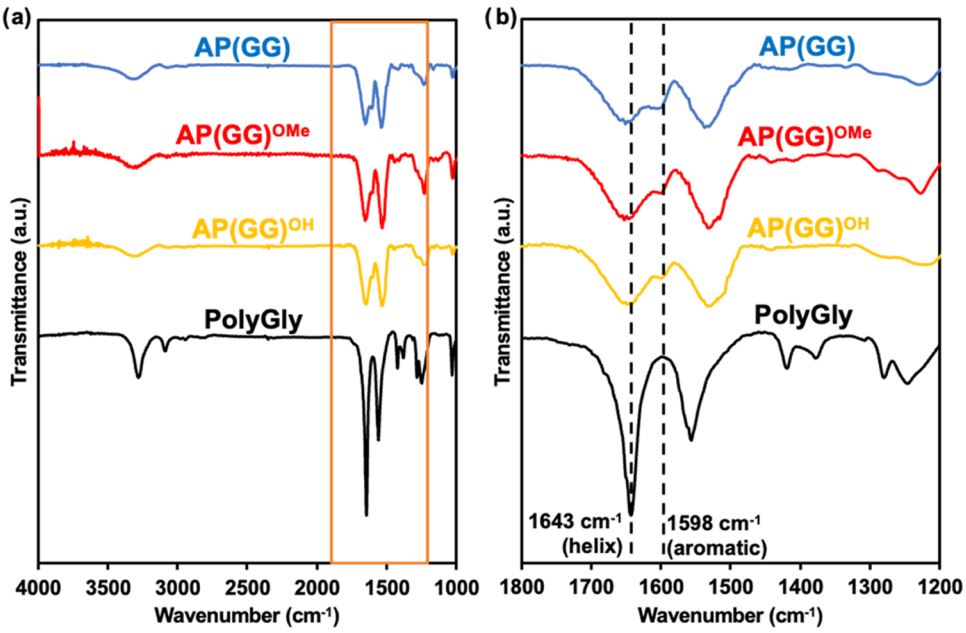

Figure 4. FT-IR spectra of AP(GG), AP(GG)^{OMe}, AP(GG)^{OH}, and PolyGly. (a) Overall spectra and (b) enlarged spectra from 1200 to 1800 cm^{-1}.

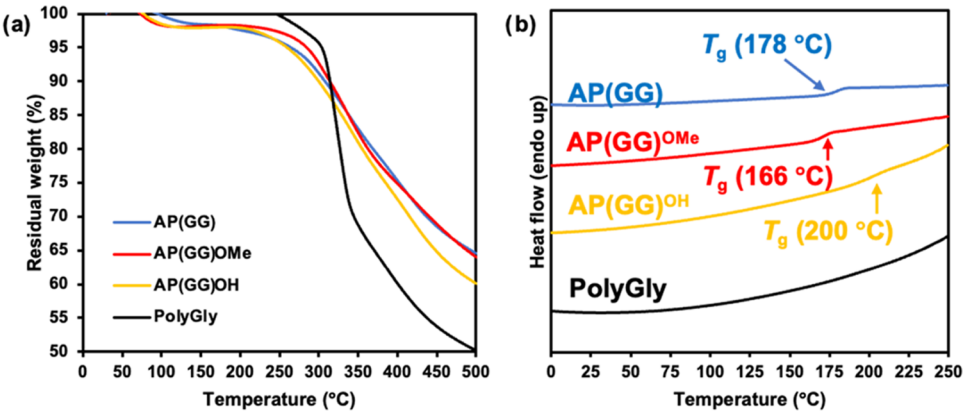

Figure 5. (a) TGA curves of AP(GG), AP(GG)^{OMe}, AP(GG)^{OH}, and PolyGly at 20 °C min^{-1} and (b) DSC profiles of AP(GG), AP(GG)^{OMe}, AP(GG)^{OH}, and PolyGly in the second heating scan at 20 °C min^{-1}.

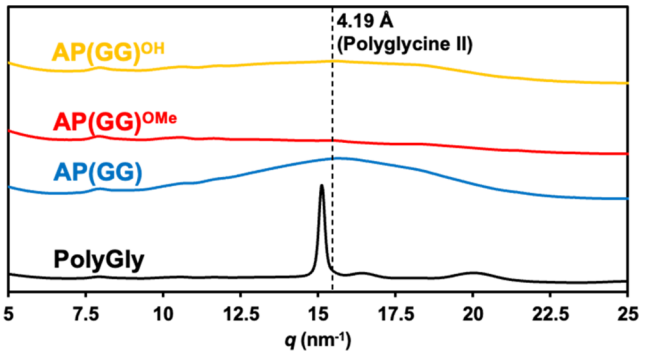

Figure 6. One-dimensional WAXD profiles of AP(GG), AP(GG)^{OMe}, AP(GG)^{OH} and PolyGly.

structure of polypeptides. PolyGly generally exhibits a helical structure, namely, polyglycine II.[21] The polyamides containing aromatic units exhibited the same amide I peak as that of PolyGly. Therefore, the polyamides encompassed a helical structure similar to that of polyglycine II.[22] In addition, another peak appeared at 1226 cm^{-1}, which was not detected in the FT-IR spectra of PolyGly. This peak was assumed to be derived from the C−N stretching vibration mode of aromatic amines.

The thermal properties of the polyamides containing aromatic units were investigated via TGA and DSC. The TGA profiles of AP(GG), AP(GG)^{OMe}, AP(GG)^{OH}, and PolyGly are shown in Figure 5a. The three polyamides containing aromatic units showed a slight weight loss of 0.5−1.5% at approximately 100 °C, which corresponded to desorption of water absorbed by the polyamides, and the 5% decomposition temperature (T_{d5}) was 285 °C for AP(GG), 298 °C for AP(GG)^{OMe} and 278 °C for AP(GG)^{OH}. Compared with those of PolyGly, the hydrophilic amine groups on the aromatic units of the polyamides likely caused greater water absorption. The char yields of the polyamides containing aromatic units after heating to 500 °C were higher than those of PolyGly. Compared with that of PolyGly, the introduction of aromatic rings into the polyamide backbones caused a greater degree of carbonization. In the case of AP(GG)^{OH}, the weight loss at 500 °C was greater than that of the other polyamides containing aromatic units. This probably

https://doi.org/10.1021/acs.macromol.4c02125
Macromolecules 2024, 57, 11658−11669

Scheme 3. Postpolycondensation of AP(GG), AP(GG)^{OMe} and AP(GG)^{OH} with PPA

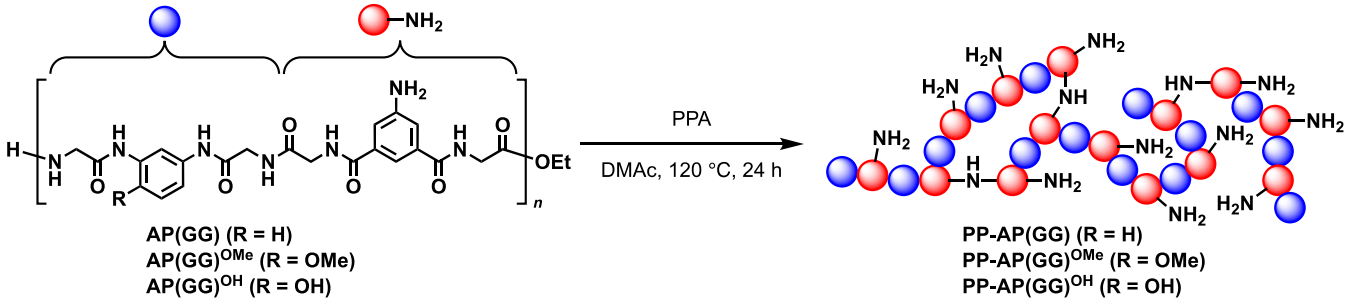

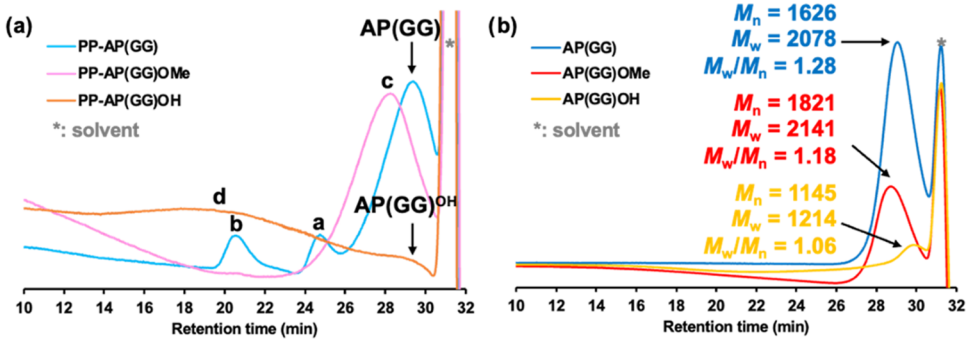

Figure 7. GPC profiles of (a) PP-AP(GG), PP-AP(GG)^{OMe} and PP-AP(GG)^{OH} synthesized via postpolycondensation with PPA and (b) AP(GG), AP(GG)^{OMe} and AP(GG)^{OH}.

Table 2. Postpolycondensation of Polyamides

prepolymer	peak[a]	M_n[b]	M_w[b]	M_w/M_n[b]
AP(GG)	a	1.63×10^4	1.76×10^4	1.08
AP(GG)	b	1.14×10^5	1.21×10^5	1.06
AP(GG)^{OMe}	c	2.59×10^3	4.65×10^3	1.79
AP(GG)^{OH}	d	7.16×10^4	3.36×10^5	4.69

[a]Peaks labeled in the GPC profiles in Figure 7. [b]Determined via GPC using polystyrene standards.

occurs because the aromatic hydroxyamide was converted into a benzoxazole at high temperatures, which liberated additional water via cyclization.

According to the DSC profiles, PolyGly, which is a typical natural polypeptide, indicated no melting point or glass transition temperature (T_g) below its degradation temperature, as shown in Figures 5b and S6. In contrast, all the polyamides containing aromatic units indicated a T_g value within the range from 166 to 200 °C in the second heating scan, indicating that these polyamides can be utilized as thermoplastic polymers. Compared with the other polyamides, AP(GG)^{OH} demonstrated a slightly higher T_g value at 200 °C, which was assumedly caused by hydrogen bonds derived from the hydroxy groups on the aromatic units. The incorporation of aromatic units affected the crystalline structure of the glycine-based polypeptide backbone, resulting in the formation of an amorphous phase. These polymers were melt-processed using a heat press to form 1 mm-thick films (Figure S8). While the polymers demonstrated thermal processability, the resulting films were hard and brittle. This indicates that the molecular redesign of the polymers, particularly targeting higher molecular weights, is necessary to achieve tougher, self-standing films.

WAXD measurements were performed to further investigate the secondary structure of the polyamides containing aromatic units. The WAXD profiles of the polyamides are shown in Figure 6. PolyGly showed a representative sharp peak at 15 nm^{-1} (4.19 Å), corresponding to the interchain distance of the hexagonal packing of the PolyGly chains in the polyglycine II crystalline phase.[21] In contrast, the series of polyamides containing aromatic units exhibited a broad peak only in the WAXD profile. In contrast to PolyGly, no sharp peak was observed, indicating that these polyamides largely exhibited an amorphous state. In our previous study, glycine-based polypeptides containing periodically aromatic units were synthesized, which demonstrated crystalline peaks similar to those in the WAXD profile of PolyGly.[7] The polyamides AP(GG), AP(GG)^{OMe}, and AP(GG)^{OH} possessed alternating GlyGly units with different N to C directions between the aromatic units because they were synthesized by AA/BB-type chemoenzymatic polycondensation. This structural difference likely caused these polyamides to adopt an amorphous state.

Since the molecular weight of these polymers prevents their utilization as materials, the molecular weight obtained via enzymatic polymerization is limited. Therefore, main chain elongation was performed through postpolycondensation using the synthesized polyamides as prepolymers. To achieve high molecular weight polymers, high-temperature polymerization is necessary to prevent the reduction in mixing efficiency caused by increased viscosity as molecular weight rises. In such cases, conventional condensing agents may decompose. Therefore, the use of polyphosphoric acid (PPA), which can withstand high-temperature polymerization, was considered advantageous.[4,8] As shown in Scheme 3, we employed PPA as a condensing agent, and the reaction was conducted at a high temperature of 120 °C under a nitrogen atmosphere.

In the GPC profiles (Figure 7), broad peaks (peaks b, c, and d) were observed for all the postpolymers in the higher-molecular-weight region compared with the prepolymers, although PP-AP(GG) and PP-AP(GG)^{OH} showed peaks

https://doi.org/10.1021/acs.macromol.4c02125
Macromolecules 2024, 57, 11658−11669

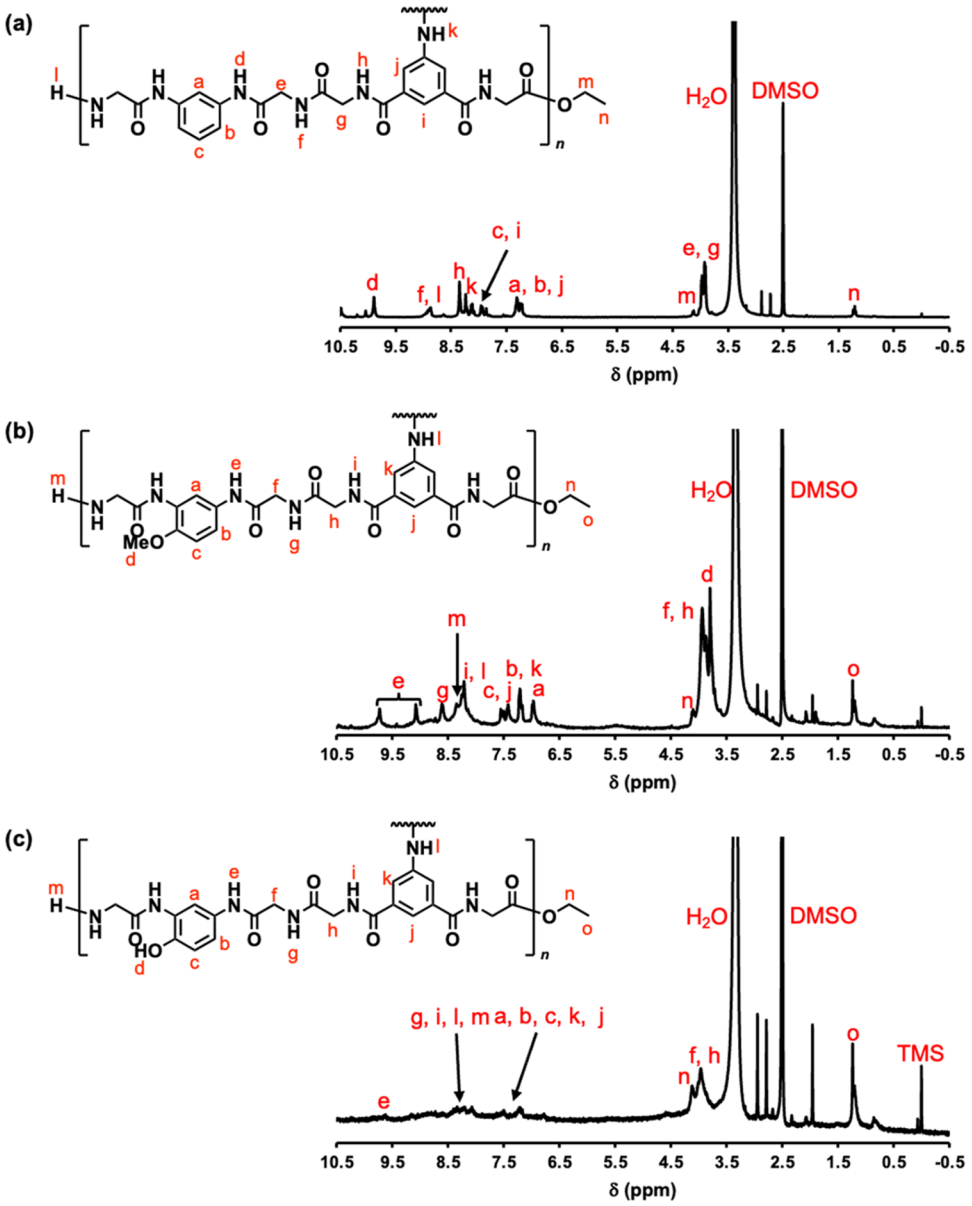

Figure 8. ^{1}H NMR spectra of (a) PP-AP(GG), (b) PP-AP(GG)^{OMe} and (c) PP-AP(GG)^{OH} in DMSO-d_6.

almost identical to those of the prepolymers. The overlapping peaks of AP(GG)^{OH} were attributed to its insolubility in common solvents, including mobile phase solvents, resulting in a saturation concentration lower than that of other prepolymers. The postcondensed polymer was precipitated at the early stages for AP(GG), causing the prepolymer to remain unreacted. In contrast, the low solubility of AP(GG)^{OH} in DMAc resulted in the remaining prepolymer. The broadening of the peak indicated that a poorly soluble networked/hyperbranched polymer was formed by the condensation between the terminal ester groups and the side-chain amino group of the Aip units. The multimodal nature of the GPC curve was likely due to the polymer becoming insoluble and precipitating in its cross-linked state during polymerization, leading to polymerization in a heterogeneous system and resulting in the production of polydisperse polymers. The polymers after postpolycondensation with branched structures have a smaller hydrodynamic radius compared to linear polymers. Therefore, the molecular weights of the postpolymers by GPC were likely underestimated when using linear PS as a standard. Specifically, in the case of AP(GG)^{OH}, the MALDI-TOF MS spectra revealed the formation of prepolymers rich in ester termini, which might cause a reaction between the ester moiety at the termini and the side-chain amino group of Aip. Therefore, PP-AP(GG)^{OH} exhibited a high M_n of 7.16 × 10^4 with a broad molecular weight distribution (M_w/M_n = 4.69). In the case of AP(GG)^{OMe}, prepolymers rich in amine termini were produced, resulting in a slight increase in the molecular weight (Table 2). Conversely, in the case of PP-AP(GG) and PP-AP(GG)^{OH}, a peak derived from the prepolymer was also detected, indicating incomplete postpolycondensation because the reactions stopped due to their low solubility.

Figure 8 shows the ^{1}H NMR spectra of the polymers after postpolycondensation. Compared with the ^{1}H NMR spectra of the prepolymers, the spectra were generally broad, and overlap due to these factors was also observed, especially on the low magnetic field. In addition, in the postcondensed polymers, the

https://doi.org/10.1021/acs.macromol.4c02125
Macromolecules 2024, 57, 11658−11669

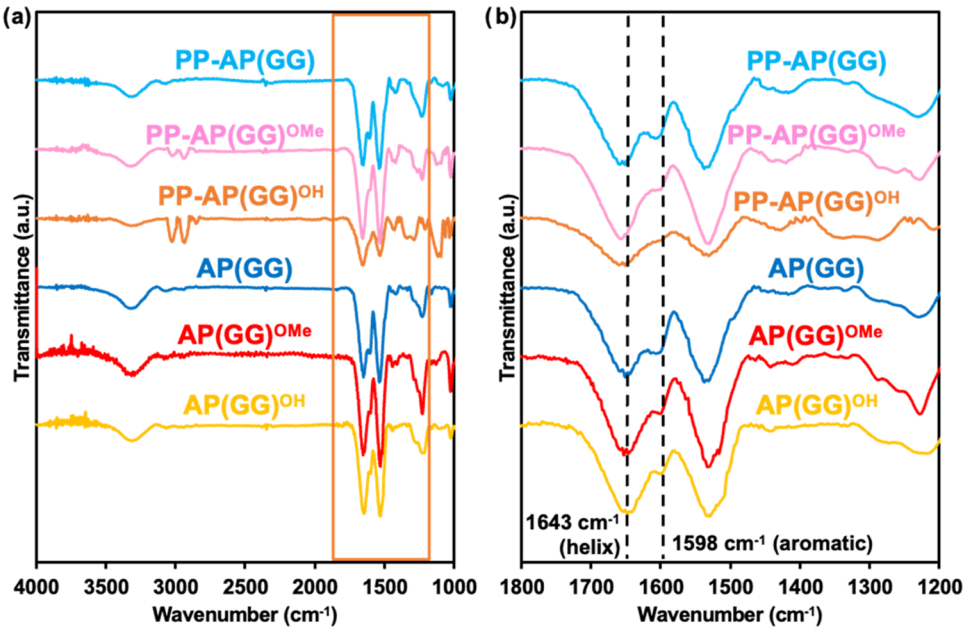

Figure 9. FT-IR spectra of PP-AP(GG), PP-AP(GG)^{OMe}, PP-AP(GG)^{OH}, AP(GG), AP(GG)^{OMe} and AP(GG)^{OH}. (a) Overall spectra from 1000 to 4000 cm^{-1}. (b) Enlarged spectra from 1,200 to 1,800 cm^{-1}.

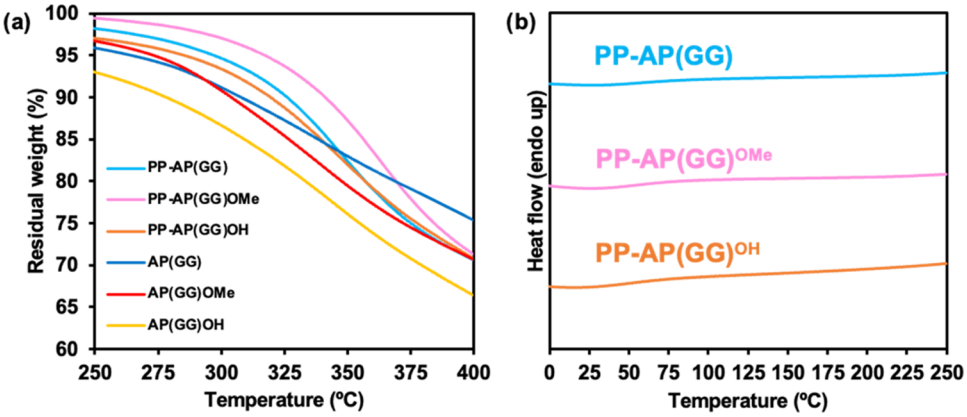

Figure 10. Thermal analysis of PP-AP(GG), PP-AP(GG)^{OMe} and PP-AP(GG)^{OH}. (a) TGA curves via heating at 20 °C min^{-1}. (b) DSC profiles after heating at 20 °C min^{-1}.

peak of the amino group of Aip was not observed at approximately 5.5 ppm but was instead observed within the amide proton region, suggesting that the network structure had progressed through amidation.

Structural analysis and thermophysical property assessment of the postpolycondensed polymer were also conducted. FT-IR analysis (Figure 9) validated the similarity of the secondary structure to that of the prepolymers. Compared with those of the prepolymers, the amide I peak slightly shifted toward higher wavenumbers, whereas the amide II peak slightly shifted toward lower wavenumbers with peak broadening. This is due to the formation of hyperbranched/networked structures by postpolycondensation.

The thermophysical properties of the polymer were subsequently investigated. The TGA curves (Figure 10a) revealed that both T_{d5} and the 10% decomposition temperature (T_{d10}) increased after postpolycondensation, which suggests improved thermal stability until decomposition. These thermal stabilities could increase with increasing molecular weight.

The DSC profiles (Figures 10b and S7) revealed the absence of T_g observed for the prepolymers within the temperature range from 0 to 250 °C for the polymers obtained by postpolycondensation. Similar to the TGA results, the formation of thermally stable networked/hyperbranched structures by postcondensation caused the disappearance of T_g.

CONCLUSIONS

In this study, polypeptides incorporating an aromatic ring in the main chain were synthesized to emulate commercially available polyamides, aiming to confer thermoplasticity, which is absent in conventional polypeptides. The enzymatic recognition was enhanced by flanking aromatic units with natural amino acids such as glycine, resulting in polyamide formation via enzymatic polycondensation between the diamine and diester monomers.

The structural analysis results suggested that the polyamides are amorphous. These results indicated that introducing aromatic rings into the main chain caused the collapse of the crystal structures derived from PolyGly. The TGA measure-

https://doi.org/10.1021/acs.macromol.4c02125
Macromolecules 2024, 57, 11658−11669

ments revealed that the obtained polyamides exhibited greater thermal stability than did PolyGly, which could be attributed to the rigid aromatic rings in the main chain. Additionally, DSC analysis revealed that glass transition occurred between 165 and 200 °C, which was not observed for crystalline PolyGly, due to the amorphous nature of these polymers.

To enhance its practicality as a polymer material, we aimed to increase the molecular weight via main chain extension via postpolycondensation with PPA. The resulting postcondensation polymer exhibited a molecular weight of approximately 16,000. The spectroscopic and thermal analysis results revealed that the postpolycondensation polymers were networked/hyperbranched structures, probably due to the branching reaction with the amino groups in the Aip units.

For future developments, evaluating the biodegradability of these polymers will enable comparisons of peptide bond-driven biodegradability levels. Further study exploring the polymer variations by substituting amino acids such as alanine or serine instead of glycine could enhance the thermal stability and processability compared to the current AP(GG) series. In addition, we aim to establish an enzymatic synthesis system that eliminates the need for organic solvents or condensing agents during monomer synthesis and postpolymerization, by applying suitable enzymatic synthetic methods. Based on the findings in this study, we will further advance research toward producing high-performance polymers with superior thermophysical properties through more environmentally friendly process.

■ ASSOCIATED CONTENT

Supporting Information

The Supporting Information is available free of charge at https://pubs.acs.org/doi/10.1021/acs.macromol.4c02125.

MALDI-TOF MS spectra of AP(GG) synthesized under various conditions (total monomer concentration, papain concentration, buffer pH and time course); and overall DSC profiles, including the first heating scan and cooling scan (PDF)

■ AUTHOR INFORMATION

Corresponding Authors

Kousuke Tsuchiya − *Department of Chemistry and Biotechnology, School of Engineering, The University of Tokyo, Tokyo 113-8656, Japan;* orcid.org/0000-0003-2364-8275; Email: ktsuchiya@gel.t.u-tokyo.ac.jp

Keiji Numata − *Department of Material Chemistry, Graduate School of Engineering, Kyoto University, Kyoto 615-8510, Japan; Biomacromolecules Research Team, RIKEN Center for Sustainable Resource Science, Wako, Saitama 351-0198, Japan;* orcid.org/0000-0003-2199-7420; Email: keiji.numata@riken.jp

Authors

Yusuke Ueno − *Department of Material Chemistry, Graduate School of Engineering, Kyoto University, Kyoto 615-8510, Japan*

Hiroyasu Masunaga − *Japan Synchrotron Radiation Research Institute, Sayo-gun, Hyogo 679-5198, Japan*

Complete contact information is available at: https://pubs.acs.org/10.1021/acs.macromol.4c02125

Author Contributions

K.T. and K.N. conceived and designed the research. Y.U. performed the experiments and analyzed the data. K.T. and H.M. performed the WAXD analysis. Y.U. and K.T. wrote the manuscript, and K.T. and K.N. edited the manuscript.

Funding

This work was supported by Grants-in-Aid from JST PRESTO Grant No. JPMJPR21N6, JST-Mirai Program Grant No. JPMJMI21EF, and JSPS KAKENHI Grant No. JP20K05636, JST COI-NEXT, and the MEXT Program: Data Creation and Utilization-Type Material Research and Development Project Grant Number JPMXP1122714694. This work was partially supported by the Asahi Glass Foundation.

Notes

The authors declare no competing financial interest.

■ REFERENCES

(1) Saric, M.; Scheibel, T. Engineering of silk proteins for materials applications. *Curr. Opin. Biotechnol.* **2019**, *60*, 213−220.

(2) Vendrely, C.; Scheibel, T. Biotechnological Production of Spider-Silk Proteins Enables New Applications. *Macromol. Biosci.* **2007**, *7* (4), 401−409.

(3) Sarkar, A.; Connor, A. J.; Koffas, M.; Zha, R. H. Chemical Synthesis of Silk-Mimetic Polymers. *Materials* **2019**, *12* (24), No. 4086.

(4) Tsuchiya, K.; Numata, K. Chemical Synthesis of Multiblock Copolypeptides Inspired by Spider Dragline Silk Proteins. *ACS Macro Lett.* **2017**, *6* (2), 103−106.

(5) Latza, V.; Guerette, P. A.; Ding, D.; Amini, S.; Kumar, A.; Schmidt, I.; Keating, S.; Oxman, N.; Weaver, J. C.; Fratzl, P.; Miserez, A.; Masic, A. Multi-scale thermal stability of a hard thermoplastic protein-based material. *Nat. Commun.* **2015**, *6* (1), No. 8313.

(6) Wright, E. R.; McMillan, R. A.; Cooper, A.; Apkarian, R. P.; Conticello, V. P. Thermoplastic Elastomer Hydrogels via Self-Assembly of an Elastin-Mimetic Triblock Polypeptide. *Adv. Funct. Mater.* **2002**, *12* (2), 149−154.

(7) Tsuchiya, K.; Kurokawa, N.; Gimenez-Dejoz, J.; Gudeangadi, P. G.; Masunaga, H.; Numata, K. Periodic introduction of aromatic units in polypeptides via chemoenzymatic polymerization to yield specific secondary structures with high thermal stability. *Polym. J.* **2019**, *51* (12), 1287−1298.

(8) Gudeangadi, P. G.; Tsuchiya, K.; Sakai, T.; Numata, K. Chemoenzymatic synthesis of polypeptides consisting of periodic di- and tri-peptide motifs similar to elastin. *Polym. Chem.* **2018**, *9* (17), 2336−2344.

(9) Okamura, T.-a.; Seno, S. Strategic Construction of Chiral Helices: Expanded Poly(l-leucine) Containing p-Phenylene Moieties. *Macromolecules* **2017**, *50* (9), 3500−3509.

(10) Ishido, Y.; Kanbayashi, N.; Okamura, T.-a.; Onitsuka, K. Synthesis of Nonnatural Helical Polypeptide via Asymmetric Polymerization and Reductive Cleavage of N−O Bond. *Macromolecules* **2017**, *50* (14), 5301−5307.

(11) Yazawa, K.; Gimenez-Dejoz, J.; Masunaga, H.; Hikima, T.; Numata, K. Chemoenzymatic synthesis of a peptide containing nylon monomer units for thermally processable peptide material application. *Polym. Chem.* **2017**, *8* (29), 4172−4176.

(12) Tsuchiya, K.; Numata, K. Chemoenzymatic Synthesis of Polypeptides for Use as Functional and Structural Materials. *Macromol. Biosci.* **2017**, *17* (11), No. 1700177.

(13) Gudeangadi, P. G.; Uchida, K.; Tateishi, A.; Terada, K.; Masunaga, H.; Tsuchiya, K.; Miyakawa, H.; Numata, K. Poly(alanine-nylon-alanine) as a Bioplastic: chemoenzymatic synthesis, thermal properties and biological degradation effects. *Polym. Chem.* **2020**, *11* (30), 4920−4927.

(14) García, J. M.; García, F. C.; Serna, F.; de la Peña, J. L. High-performance aromatic polyamides. *Prog. Polym. Sci.* **2010**, *35* (5), 623−686.

(15) Maniar, D.; Hohmann, K. F.; Jiang, Y.; Woortman, A. J. J.; van Dijken, J.; Loos, K. Enzymatic Polymerization of Dimethyl 2,5-Furandicarboxylate and Heteroatom Diamines. *ACS Omega* **2018**, *3* (6), 7077−7085.
(16) Jiang, Y.; Maniar, D.; Woortman, A. J. J.; Loos, K. Enzymatic synthesis of 2,5-furandicarboxylic acid-based semi-aromatic polyamides: enzymatic polymerization kinetics, effect of diamine chain length and thermal properties. *RSC Adv.* **2016**, *6* (72), 67941−67953.
(17) Ageitos, J. M.; Yazawa, K.; Tateishi, A.; Tsuchiya, K.; Numata, K. The Benzyl Ester Group of Amino Acid Monomers Enhances Substrate Affinity and Broadens the Substrate Specificity of the Enzyme Catalyst in Chemoenzymatic Copolymerization. *Biomacromolecules* **2016**, *17* (1), 314−323.
(18) Sangeetha, K.; Abraham, T. E. Chemical modification of papain for use in alkaline medium. *J. Mol. Catal. B: Enzym.* **2006**, *38* (3), 171−177.
(19) Sluyterman, L. A. Æ.; De Graaf, M. J. M. The activity of papain in the crystalline state. *Biochim. Biophys. Acta, Enzymol.* **1969**, *171* (2), 277−287.
(20) Qin, X.; Xie, W.; Tian, S.; Cai, J.; Yuan, H.; Yu, Z.; Butterfoss, G. L.; Khuong, A. C.; Gross, R. A. Enzyme-triggered hydrogelation via self-assembly of alternating peptides. *Chem. Commun.* **2013**, *49* (42), 4839−4841.
(21) Qin, X.; Khuong, A. C.; Yu, Z.; Du, W.; Decatur, J.; Gross, R. A. Simplifying alternating peptide synthesis by protease-catalyzed dipeptide oligomerization. *Chem. Commun.* **2013**, *49* (4), 385−387.
(22) Crick, F. H. C.; Rich, A. Structure of Polyglycine II. *Nature* **1955**, *176*, 780−781.

https://doi.org/10.1021/acs.macromol.4c02125
Macromolecules 2024, 57, 11658−11669